

Institut für Reaktorwerkstoffe

KERNFORSCHUNGSANLAGE JÜLICH

des Landes Nordrhein-Westfalen - e. V.

PRELIMINARY RESULTS ON RADIATION  
DAMAGE IN VARIOUS GRAPHITES

von

M. Beutell, E. Fitzer, R. Gain und O. Vohler

Jül - 121 - RW

September 1963

**Berichte der Kernforschungsanlage Jülich - Nr. 121**  
**Institut für Reaktorwerkstoffe Jül - 121 - RW**

Dok.: GRAPHITE  
NEUTRON IRRADIATION  
X-RAY IRRADIATION

DK: 546.26-162 : 621.039.556 : 626.179.152

Zu beziehen durch: ZENTRALBIBLIOTHEK der Kernforschungsanlage Jülich,  
Jülich, Bundesrepublik Deutschland

*Reprinted from*  
*“Proceedings of the Fifth Carbon Conference”*  
*Volume II*

PERGAMON PRESS

OXFORD · LONDON · NEW YORK · PARIS

1963

*Printed in Great Britain by J. W. Arrowsmith Ltd., Bristol 3*

# PRELIMINARY RESULTS ON RADIATION DAMAGE IN VARIOUS GRAPHITES

M. BEUTELL, E. FITZER, R. GAIN, and O. VOHLER

*Research Laboratory, Siemens-Planwierke AG., Meitingen bei Augsburg*

and

*Institut für Reaktorwerkstoffe der Kernforschungsanlage Jülich, Aachen, Germany*

(Manuscript received October 3, 1961)

Preliminary results of a broad irradiation program on graphite are reported. Within this program graphites of different degree of graphitization, given by the different graphitizability of the filler materials, have been studied. The irradiations were carried out with neutron doses up to  $5 \times 10^{21}$  nvt at temperatures ranging from 70° to 700°C. The changes in physical properties such as lattice distance, macroscopic dimensions, density, thermal and electrical conductivity, magnetic susceptibility, coefficient of thermal expansion, mechanical strength and others are reported, with special emphasis on the influence of the degree of graphitization.

## I. INTRODUCTION

A broad irradiation program for graphite, sponsored by the Ministry of Atomic Affairs, is being carried out in the Federal Republic of Germany.

Within this program graphites of different degrees of graphitization are being studied under controlled irradiation conditions. This different degree of graphitization of the specimens was obtained not by a different heat treatment, but only by the different graphitizability of the raw materials. In all cases the same binder was used, and all samples were graphitized exactly in the same manner.

Apart from a few quotations in the literature as to the raw material of various irradiated graphites<sup>1</sup> there are no systematic investigations on the influence of different filler materials on the irradiation behavior of graphites.

All irradiations reported in this paper were carried out in the GETR at Vallecitos.

<sup>1</sup> W. K. Woods, L. P. Bupp, and J. F. Fletcher, *Proc. First United Nations Conf. on Peaceful Uses of Atomic Energy* 7, 455 (1956); R. E. Nightingale, J. M. Davidson, and J. F. Fletcher, *Proc. Second United Nations Conf. on Peaceful Uses of Atomic Energy* 7, 295 (1959), *Proc. Fourth Carbon Conf.* Pergamon Press (1960), p. 599.

Neutron doses ranging from  $1 \times 10^{19}$  up to  $5 \times 10^{21}$  with energies greater than 0.17 eV were applied at temperatures between 70 and 700°C. For high neutron doses ( $1 \times 10^{21}$ – $5 \times 10^{21}$  nvt > 0.17 eV) positions in the core of the reactor were chosen, whereas lower doses ( $1 \times 10^{19}$ – $2 \times 10^{20}$  nvt) were irradiated in the pool. The neutron doses were determined by calculations according to the three-group-theory and by measurements with sulphur-monitors.

In the core exists a neutron spectrum of very high energy with about 55% of an energy greater than 180 keV, whereas in the pool positions only 43% show an energy greater than 180 keV. This fact is important, because only the group with neutron energies higher than 180 keV, determined by the three-group-theory, is responsible for the radiation damage in graphite.

The irradiation temperatures were measured by special thermo-elements or temperature monitors.

## II. IRRADIATED GRAPHITE TYPES

To save space in the irradiation capsules it was tried for the first time to use very small samples having dimensions of  $5 \times 5 \times 45$  mm cut out in the appropriate directions.

In order to perform measurements on these small samples new methods had to be developed. In all cases, however, the variations of the data caused by the small sample-size are smaller than those caused by the irregularities of the temperature and flux conditions.

Since the materials were chosen according to their different degree of graphitization, the definition of this quantity has basic importance. The degree of graphitization is defined by the degree of crystalline order, which is expressed by means of X-ray data as  $c$ -spacing and crystallite size. In technical carbon products, however, difficulties arise because they contain areas of well and poorly graphitized material next to each other. In the measurement of the lattice spacing, however, the perfectly crystallized parts contribute disproportionately more as will be shown later.

Besides using X-ray methods there are technical properties such as electrical resistance and thermal expansion for characterizing the degree of graphitization of the specimens. All these bulk properties, however, are sensitive to the macrostructure such as porosity, orientation, defects, etc.

Another technique which has been used successfully for several decades is the measurement of the density of the finely powdered graphite. Up to now this method is seldom reported in the literature on artificial graphite. In our case this quantity was used successfully in order to interpret the irradiation experiments.

In addition an X-ray method was developed in order to determine quickly the degree of graphitization even of highly heterogeneous graphitized products. The method is explained in Fig. 1 by means of a typical 002 line profile for a mixture consisting of well and poorly graphitized components. For technical graphites, however, the two components of the line are hardly separated. The poorly graphitized portions are noticeable

only by a broadening or rising of the flank of the line at low scattering angles.

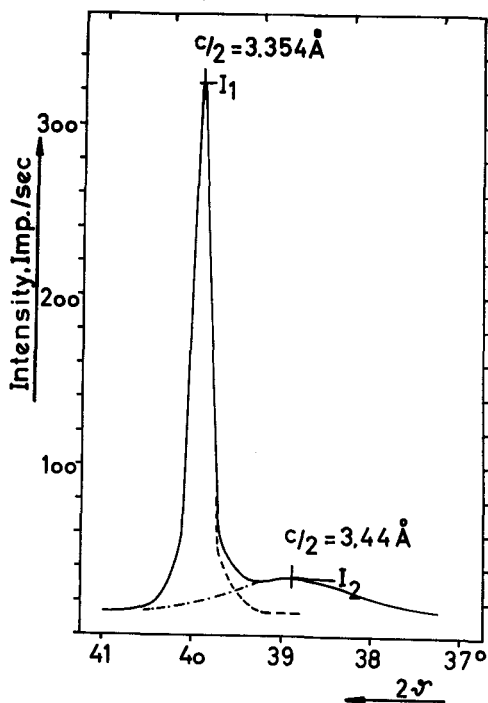


Fig. 1. The (002) line of a mixture of well and poorly graphitized carbon components.

For the above mentioned determination of the degree of graphitization the 002 line is divided into two theoretical curves, one for the ordered and one for the disordered, state as defined by Franklin<sup>2</sup>. The ratio of the two areas is a relative criterion for the degree of graphitization. On the other hand, it is not necessary to integrate the areas, it is sufficient to take the ratio of the intensities  $I_1$  and  $I_2$  of the two theoretical peaks. The actual measurement is very simple, because it is necessary only to determine the intensities at the scattering angles of the layer distances 3.44 and 3.35 Å. The intensity ratio is called I.V.-value ("Intensitäts-Verhältnis").

<sup>2</sup> R. E. Franklin, *Acta Cryst.* 4, 253 (1951).

Special types WW Incr. degr. of graph WW

TABLE I

*Physical Properties of the Graphite Samples (Unirradiated)*  
(Grain size < 0.75 mm)

Samples	I.V.-value	c-spacing Å	Real density, g/cm <sup>3</sup>	Bulk density, g/cm <sup>3</sup>	Coefficient of thermal expansion 1/°C × 10 <sup>6</sup>			
					with grain	across grain	cubical	
Incr. degr. of graph. ↑	1	56.0	6.721	2.247	1.70	1.10	3.50	8.10
	2	33.9	6.726	2.224	1.67	2.45	3.30	9.05
	3	28.7	6.731	2.200	1.60	2.05	4.30	10.65
	4	18.8	6.749	2.180	1.70	3.95	4.80	13.55
	5	6.8	6.773	2.160	1.80	5.85	6.05	17.95
Special types	6	37.1	6.728	2.233	1.70	2.80	3.50	9.80
	7	34.2	6.722	2.228	1.55	2.55	5.35	13.25
	8	31.0	6.737	2.217	1.70	1.95	3.45	8.85

Table I shows some physical properties of the materials in the unirradiated state. The samples 1-5 were manufactured by the same technique, using the same binder and the same grain size distribution, the only difference being the quality of coke used. The decrease of the I.V.-value and the density as well as the increase in lattice distance and thermal expansion coefficient from group 1 to group 5 is shown.

In addition to the specimens 1-5, special types (6-8) were irradiated. These grades cannot be arranged in a proper order in this scheme, because their binders differ from those used in group 1-5, and in addition to that they were graphitized under different conditions. Out of these, group 6 and 8 represent improved commercial reactor grade graphites.

Figure 2 shows microphotographs of 6 different samples used for irradiation. It is well known that the pattern of a polished

section under polarized light gives a good information about the graphitizability of the material. The larger the regions of equal anisotropy, the easier graphitizable are the raw materials. The first row contains the easily graphitizable raw materials No. 1, 6 and 2 and the second row the more poorly graphitizable ones No. 3, 4 and 5 which show clearly the smaller regions of equal anisotropy. The graphitizability decreases from group 1 over 6 and 2 to group 5, as easily can be recognized on the microphotographs.

Figure 3 shows some bulk properties of the specimens which were irradiated. They are arranged according to their degree of graphitization using the I.V.-value for the abscissa. The same graphic representation will be used to discuss the irradiation results. Here these bulk properties are shown which can be used for technical characterization of the graphitization. There is good correlation of the

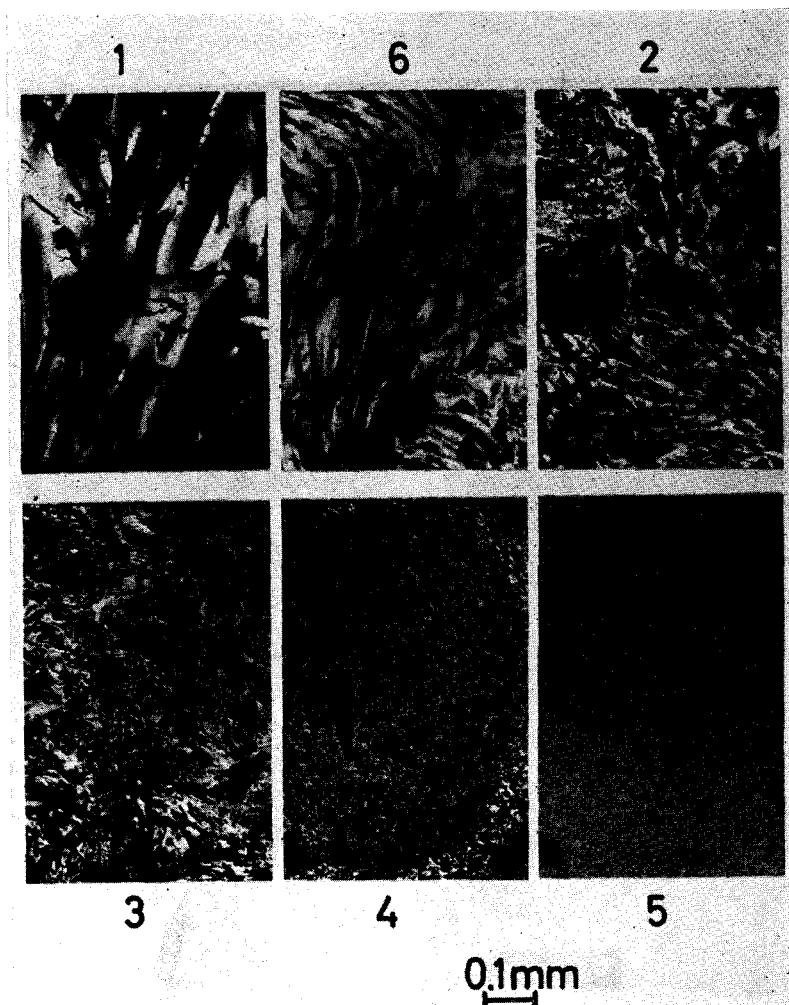


FIG. 2. Microphotographs of the different cokes used for the samples 1-6.

thermal and the electrical conductivity  $\lambda$  and  $\rho$  in direction of the grain as well as the cubical thermal expansion  $\beta$  with the degree of graphitization. Only the properties across the grain do not fit so well into this classification according to the degree of graphitization, owing to the influence of the macrostructure.

In addition, the magnetic susceptibility  $\chi$ , a measure of the crystallite size, is shown.

### III. IRRADIATION RESULTS

First the preliminary irradiation results

will be discussed as functions of the irradiation doses.

#### A. *I.V.-Value*

Figure 4 shows the variation of the *I.V.*-value as a function of neutron irradiation. It can be seen, that the graphitic areas are destroyed rapidly. At irradiation temperatures below 70°C (solid lines) almost the same final value is reached for all the various samples after a dose of  $2 \times 10^{20}$  nvt. That is caused by the *c*-spacing becoming greater than 3.44 Å in all crystallites.

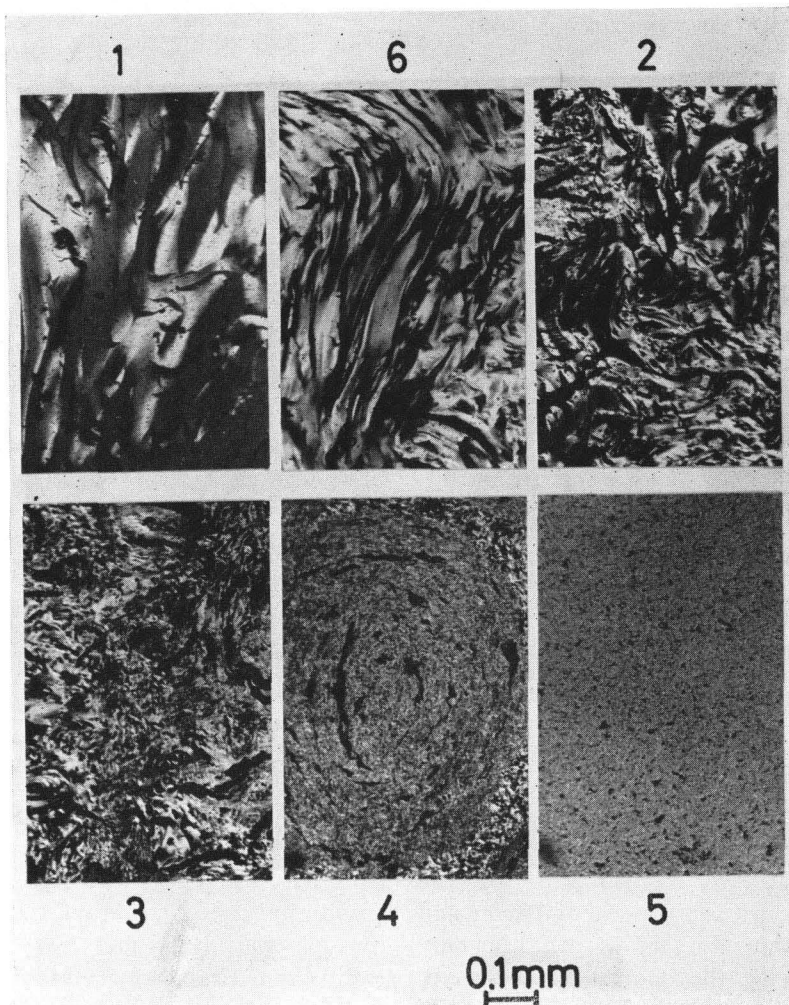


FIG. 2. Microphotographs of the different cokes used for the samples 1-6.

thermal and the electrical conductivity  $\lambda$  and  $\rho$  in direction of the grain as well as the cubical thermal expansion  $\beta$  with the degree of graphitization. Only the properties across the grain do not fit so well into this classification according to the degree of graphitization, owing to the influence of the macrostructure.

In addition, the magnetic susceptibility  $\chi$ , a measure of the crystallite size, is shown.

### III. IRRADIATION RESULTS

First the preliminary irradiation results

will be discussed as functions of the irradiation doses.

#### A. *I.V.-Value*

Figure 4 shows the variation of the *I.V.*-value as a function of neutron irradiation. It can be seen, that the graphitic areas are destroyed rapidly. At irradiation temperatures below 70°C (solid lines) almost the same final value is reached for all the various samples after a dose of  $2 \times 10^{20}$  nvt. That is caused by the *c*-spacing becoming greater than 3.44 Å in all crystallites.



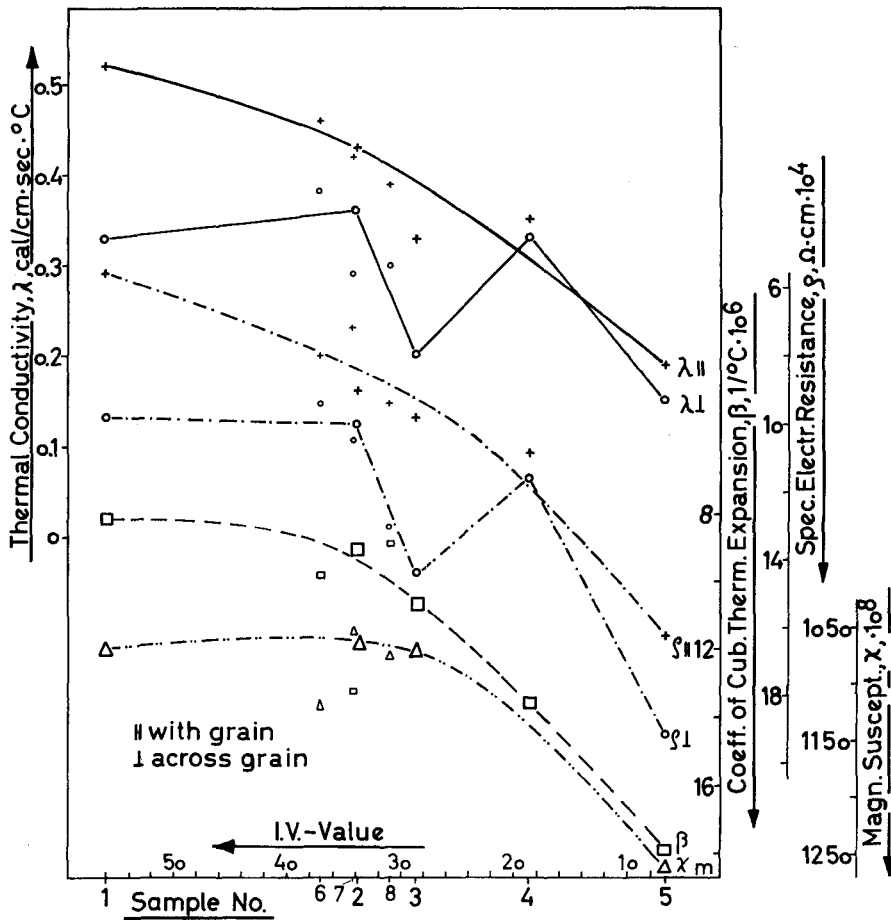


FIG. 3. The dependence of the thermal conductivity  $\lambda$ , the specific electrical resistance  $\rho$ , the coefficient of cubical thermal expansion  $\beta$ , and the magnetic susceptibility  $\chi$  of the un-irradiated samples on the degree of graphitization.

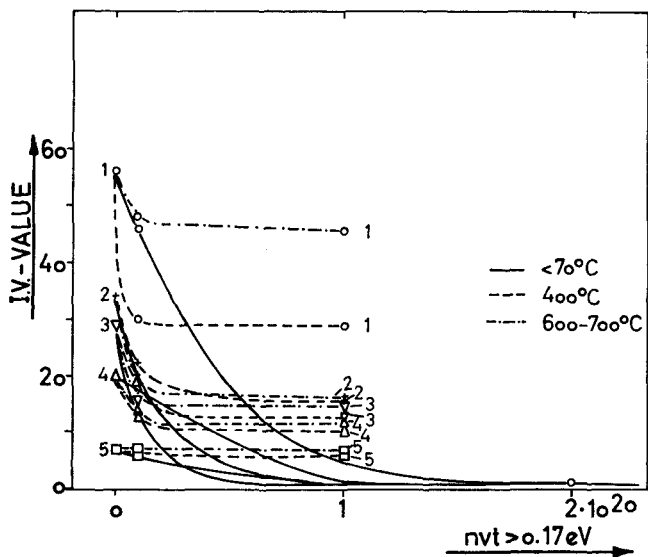


FIG. 4. Variation of the (002) intensity factor (I.V. value) with neutron irradiation.

We have found that the thermal conductivity is also leveling out at the same irradiation conditions.

At higher irradiation temperatures an equilibrium is reached because of the partial healing out at a dose as low as  $10^{19}$  nvt.

### B. *C-Spacing*

It is well known that the layer spacing is increased by neutron irradiation. In Fig. 5

found that a minimum crystallite size is reached at almost the same dose.

A correlation of alternate *c*-spacing with the degree of graphitization was not found. The smallest crystallites, however, seem to occur in those samples which were best graphitized before irradiation.

### C. *Magnetic Susceptibility*

The magnetic susceptibility is a measure

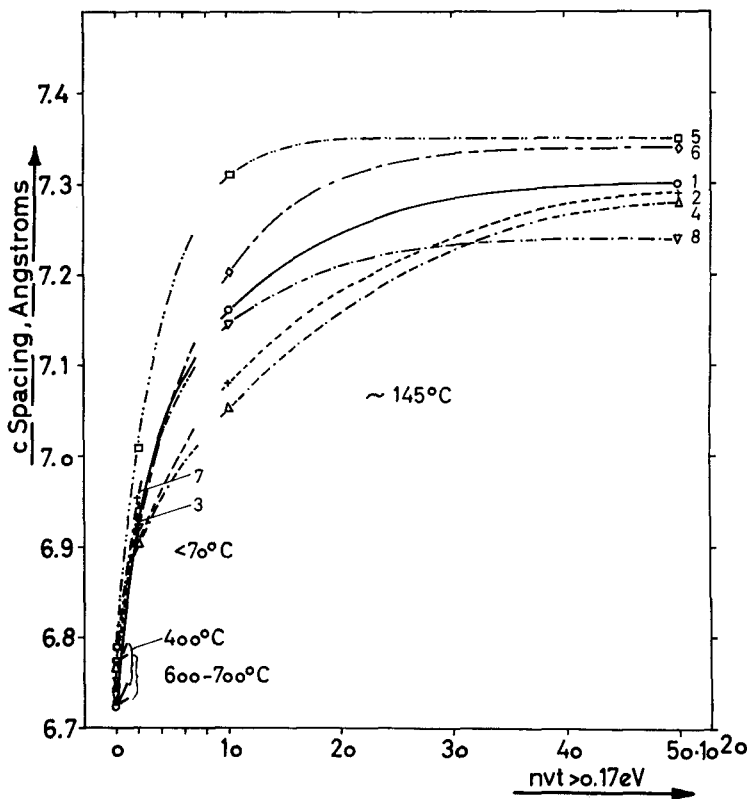


Fig. 5. Variation of *C*-spacing with neutron irradiation.

the dependence of the *c*-spacing upon the dose is shown. The lines are interrupted, because at lower irradiation doses the temperature was  $< 70^\circ\text{C}$ , at more intensive irradiation it was increased to about  $145^\circ\text{C}$ . At this temperature the layer spacing does not reach a final value before  $2 \times 10^{21}$ . From crystallite size measurements, it was

for the carrier population. Therefore its decrease shows in an excellent way the change in carrier population. Furthermore we have found that there is a certain connection with the destruction of the crystallites by neutron irradiation as determined by X-ray data. At the mentioned irradiation conditions the magnetic susceptibility reaches

a final value for all samples around the same dose as the lattice distance (Fig. 6).

#### D. Density and Pore Volume

The so-called real density determined on finely powdered samples with xylene is decreased largely by irradiation (Fig. 7). Under the irradiation conditions used, a saturation value seems to be reached at  $3 \times 10^{21}$  nvt. With some samples the density of the powder is diminished to  $1.9 \text{ g/cm}^3$ . In general, those samples which had a high density before irradiation show also a higher density after irradiation.

In addition to the determination by xylene displacement the real density was evaluated by helium. The results are compared in Table II. The differences are only in the order of  $10^{-3}$ – $3 \times 10^{-2} \text{ g/cm}^3$ , therefore the helium density is not considered in Fig. 7.

For a better understanding of the irradiation damage within a graphite it seems to be useful to discuss the variation of the pore volume. In carbon technology "pore volume" means the volume of the body which is free of carbon according to calculations based on the difference of bulk density and real density.

In the following we will call this magnitude the "bulk pore volume". Obviously the bulk pore volume is not equal to the total pore volume, because even in the powdered state graphite samples contain micropores, which are inaccessible to liquids and gases, as well as lattice defects representing a part of the total pore volume too, i.e. a space not filled with carbon atoms.

From X-ray data it is known that a perfect graphite single-crystal shows a density of  $2.266 \text{ g/cm}^3$ . For various irradiated and unirradiated graphites the actual X-ray

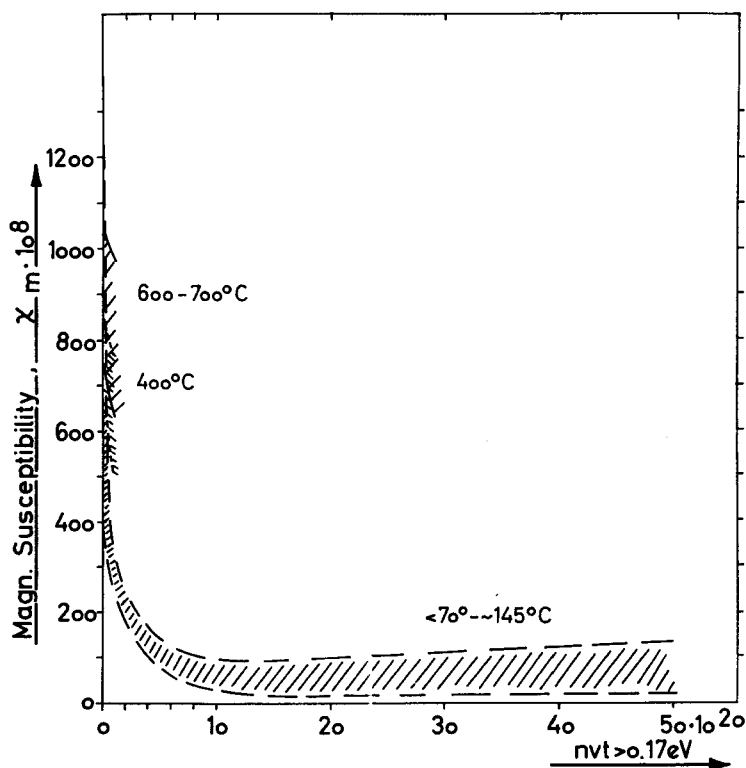


FIG. 6. Variation of the magnetic susceptibility with neutron irradiation.

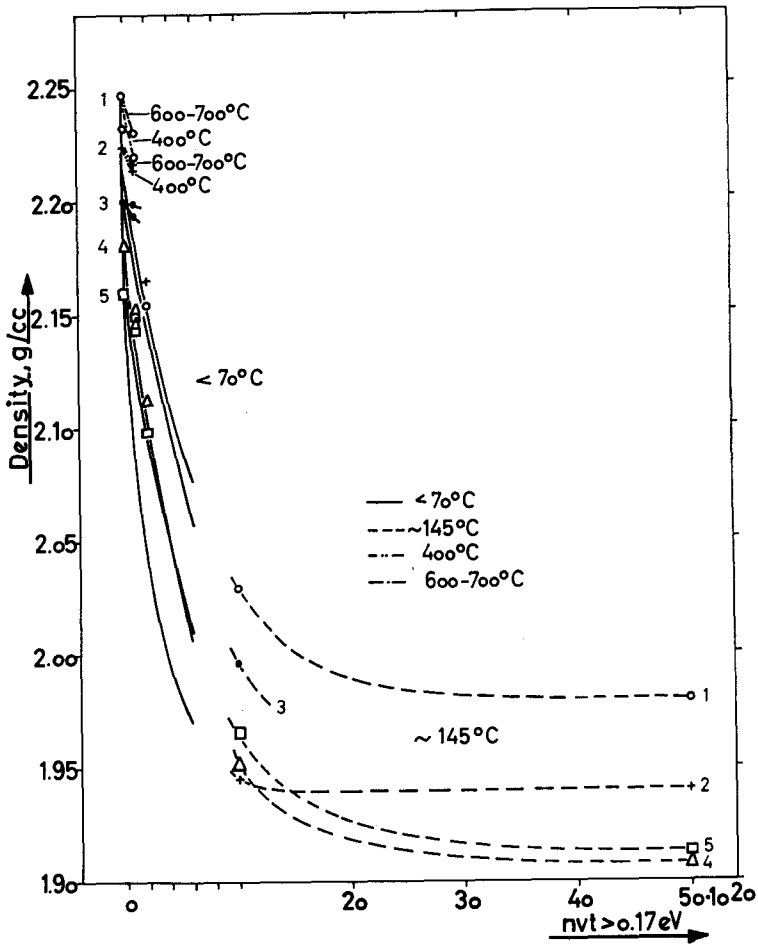


Fig. 7. Variation of the real density of graphite samples with neutron irradiation.

density can be determined from measured lattice constants.

The difference between the theoretical lattice density and the X-ray density enables us to determine the extent of the lattice defects quantitatively. This difference is caused by deviations of the layer spacing from a value of 3.354 Å as well as by spaces between the crystallites, by dislocations, distortions or extraneous atoms in the lattice.

The real density experimentally determined by helium or xylene displacement differs from the X-ray density by the micropore volume which is inaccessible to liquids and gases.

According to this definition the total pore volume is composed of the sum of the bulk

pore volume + the volume of inaccessible micropores + the space of lattice defects.

Table III shows the data of the densities (IIIa) as well as a comparison of these pore volumes of the various graphites in the original state and after an irradiation of  $5 \times 10^{21}$  nvt (IIIb). From this table it can be seen that the bulk pore volume is decreased by this intensive irradiation, whereas the volume of the inaccessible pores and to a greater extent the space of lattice defects are increased. The lattice defects reach in almost all cases a final value of about 6% by volume. The volume of the inaccessible micropores in the irradiated state depends largely on the structure of the original

TABLE II

*Variation of Real Density (determined by xylene and helium displacement) by Neutron Irradiation*

Sample	Real density, g/cm <sup>3</sup>									
	unirradiated		after $1 \times 10^{19}$ nvt at 70°C		after $2 \times 10^{20}$ nvt at 70°C		after $1 \times 10^{21}$ nvt at 145°C		after $5 \times 10^{21}$ nvt at 145°C	
	Xylene	Helium	Xylene	Helium	Xylene	Helium	Xylene	Helium	Xylene	Helium
1	2.247	2.245	2.232	2.235	2.154	2.184	2.029	2.039	1.980	1.996
2	2.224	2.220	2.204	2.212	2.165	2.156	1.945	1.954	1.940	1.952
3	2.200	2.214	2.191	2.206	2.149	2.140	1.996	1.990	(1.94)	—
4	2.180	2.174	2.132	2.128	2.112	2.119	1.951	1.953	1.908	1.922
5	2.160	2.157	2.128	2.142	2.098	2.098	1.965	1.974	1.913	1.933
6	2.233	2.221	2.215	2.205	2.168	2.145	1.931	1.924	—	—
7	2.228	2.225	2.221	2.209	2.158	2.148	—	—	—	—
8	2.217	2.218	2.203	2.203	2.156	2.143	2.012	2.042	1.906	1.937

Sample	Real density, g/cm <sup>3</sup>							
	after $1 \times 10^{19}$ nvt at 400°C		after $1 \times 10^{20}$ nvt at 400°C		after $1 \times 10^{19}$ nvt at 600–700°C		after $1 \times 10^{20}$ nvt at 600–700°C	
	Xylene	Helium	Xylene	Helium	Xylene	Helium	Xylene	Helium
1	2.232	2.243	2.230	2.232	2.223	2.229	2.220	2.226
2	2.221	2.224	2.215	2.214	2.218	2.233	2.216	2.220
3	2.196	2.205	2.194	2.203	2.188	2.212	2.199	2.197
4	2.155	2.162	2.152	2.151	2.157	2.164	2.146	2.152
5	2.140	2.164	2.149	2.120	2.142	2.148	2.143	2.143
6	2.223	2.226	2.217	2.218	2.219	2.209	2.219	2.217
7	2.213	2.215	—	—	2.215	2.211	—	—
8	2.215	2.216	2.217	2.197	2.217	2.209	2.209	2.219

sample and ranges between 4 and 12% by volume.

#### E. Wigner Growth

The dimensional changes with neutron doses shown in Fig. 8 confirm the data described in the literature. Samples prepared from well graphitized coke show a shrinking along the grain and expansion across the grain, e.g. specimen No. 1, the best graphitized and most anisotropic one. By looking on the samples 4 and 5 we see that the Wigner growth increases inversely with the degree of graphitization, but for both samples the expansion is about the same in both directions (small anisotropy).

The irradiation program at high temperature will be continued in order to study shrinkage effects.

In Fig. 9 the increase in volume is plotted for various neutron doses and irradiation temperatures as a function of the degree of graphitization of the samples (compare with Fig. 3). It is interesting to see that short time irradiations below 400°C do not yet show a definite dependence. Intensive irradiation at 145°C, however, indicates that volume expansion is not dependent in a simple way on graphitization. There is a distinct minimum volume change with the medium graphitized specimens whereas the best-graphitized and especially the poorest

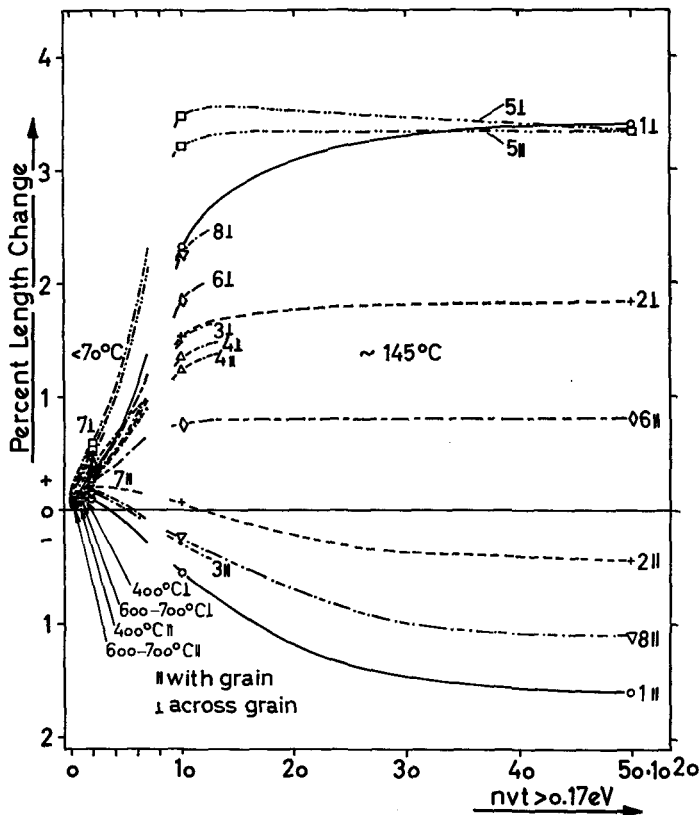


FIG. 8. Dimensional changes of graphites with neutron irradiation.

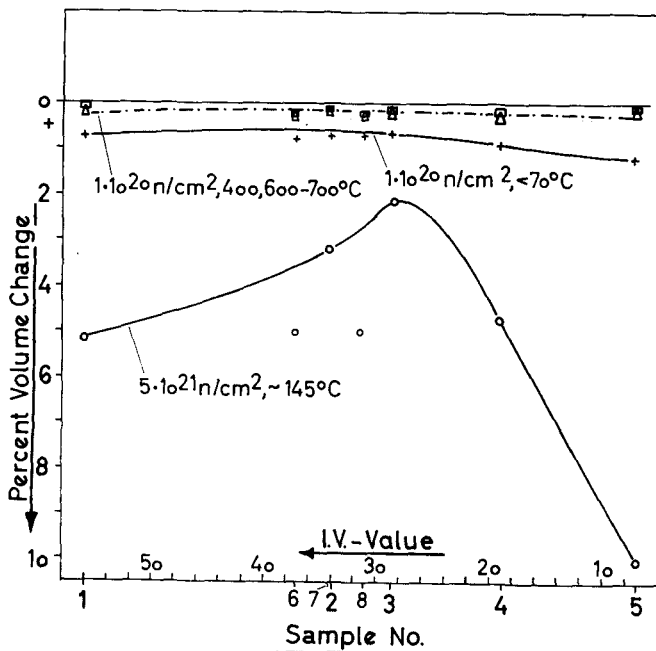


FIG. 9. Volume change of graphites by neutron irradiation.

TABLE III

(a) Variation of X-ray Density, Real Density, and Bulk Density by Irradiation with  $5 \times 10^{21}$  nvt  $> 0.17$  eV at 145°C

Sample	c-spacing Å		X-ray density, g/cm <sup>3</sup>		Real density g/cm <sup>3</sup>		Bulk density, g/cm <sup>3</sup>		
	original	irradiated	original	irradiated	original	irradiated	original	irradiated	
Incr. degr. of graph. ↑	1	6.721	7.30	2.262	2.082	2.247	1.980	1.70	1.61
	2	6.726	7.29	2.260	2.085	2.224	1.940	1.67	1.62
	3	6.731	(7.30)	2.258	(2.082)	2.200	(1.94)	1.60	1.57
	4	6.749	7.28	2.252	2.088	2.180	1.908	1.70	1.62
	5	6.773	7.35	2.244	2.068	2.160	1.913	1.80	1.62
Spec. types	6	6.728	7.34	2.259	2.071	2.233	—	1.70	1.62
	7	6.722	(7.31)	2.261	(2.079)	2.228	—	1.55	1.48
	8	6.737	7.24	2.256	2.099	2.217	1.906	1.70	1.62

(b) Variation of Pore Volumes by Irradiation with  $5 \times 10^{21}$  nvt  $> 0.17$  eV at 145°C

Sample	Total pore volume, %		X-ray pore volume, %		Volume of lattice defects, %		Volume of inaccessible micropores, %		Bulk pore volume, %	
	original	irradiated	original	irradiated	original	irradiated	original	irradiated	original	irradiated
1	25.0	28.9	24.9	22.7	0.1	6.2	0.5	4.0	24.4	18.7
2	26.3	28.5	26.1	22.3	0.2	6.2	1.2	11.8	24.9	16.5
3	29.3	30.7	29.1	(24.6)	0.3	(6.1)	1.8	(5.5)	27.3	(19.1)
4	25.0	28.5	24.5	22.4	0.5	6.1	2.5	7.3	22.0	15.1
5	20.5	28.5	19.8	21.7	0.7	6.8	3.1	6.3	16.7	15.4
6	25.0	28.5	24.7	21.8	0.3	6.7	0.8	—	23.9	—
7	31.6	34.7	31.4	(28.8)	0.2	(5.9)	1.0	—	30.4	—
8	25.0	28.5	24.6	22.8	0.4	5.7	1.2	7.8	23.4	15.0

graphitized specimens show maximum volume expansion.

Based on this knowledge we assume that the feasibility of special graphite types which will suffer only minimum changes in volume under irradiation can be estimated.

It is remarkable that the increase in volume and the coefficient of thermal expansion show no leveling out after irradiation.

#### F. Thermal Conductivity

In Fig. 10 the variation of thermal conductivity is plotted as a function of neutron dose. The final minimum conductivity is reached at  $2 \times 10^{20}$  nvt, at the same dose at which the lattice distance of the disordered

state of 3.44 Å is obtained in all crystallites. Contrary to electrical resistance, further lattice distortion causes here only small variations.

In order to elucidate the effect of leveling out by neutron irradiation in Fig. 11 the behavior of the thermal conductivity is plotted as a function of the graphitization for various irradiation doses. Whereas in the unirradiated state (especially along the grain direction) the thermal conductivity increases considerably with increasing degree of graphitization, the difference is becoming very small after neutron doses as small as  $1 \times 10^{19}$  nvt at 70°C, and it vanishes completely at higher doses.

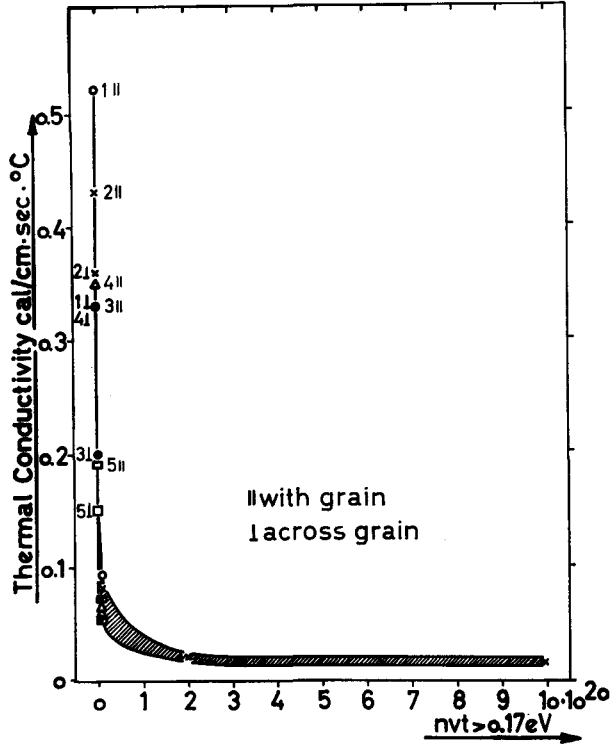


FIG. 10. Variation of the thermal conductivity of parallel and perpendicular cut graphite samples with neutron irradiation at 70°-145°C.

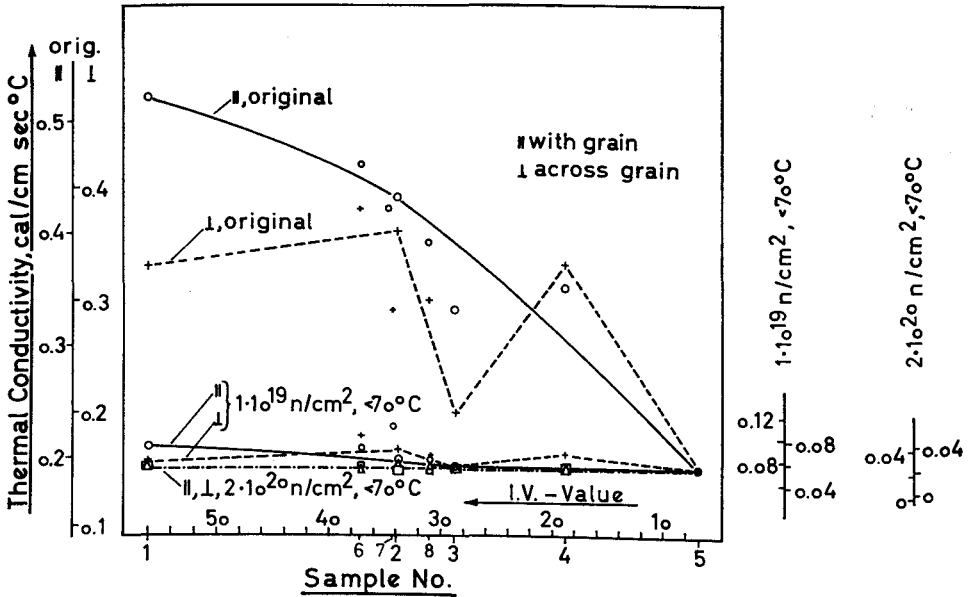


FIG. 11. Decrease of the thermal conductivity of different graphite samples after neutron irradiation at < 70°C.



In Fig. 11, lines have been drawn to connect those values of thermal conductivity obtained under the same irradiation conditions. For reasons of clarity, all curves have been drawn to start at one point, the point of sample No. 5. The scale of the ordinate is the same for all irradiation conditions but it is shifted with respect to the origin. The leveling out of the thermal conductivity can be seen at an irradiation dose as small as  $1 \times 10^{19}$  nvt at  $70^\circ\text{C}$ . It is interesting that the anisotropic behavior of the thermal conductivity is transformed into a very isotropic conductance. Even after a short irradiation, there remain almost no differences between the principal directions.

G. Electrical Resistance

The specific electrical resistance shows in principle a similar tendency (Fig. 12). At

$5 \times 10^{21}$  nvt. In contrast, the high temperature irradiations at a dose of  $1 \times 10^{20}$  nvt show an increase in the differences of the electrical resistance between the various graphites, which can be seen by the steep slope of the line in the range of low degrees of graphitization.

H. Thermal Expansion

The coefficient of thermal expansion of irradiated samples was also determined. The results are plotted against the degree of graphitization in Fig. 13. Naturally these measurements could only be carried out below the irradiation temperature in order to avoid annealing of the radiation damages.

There was one very interesting result: The cubic expansion coefficient for well-graphitized samples seems to increase after long time exposure, for poorly graphitized

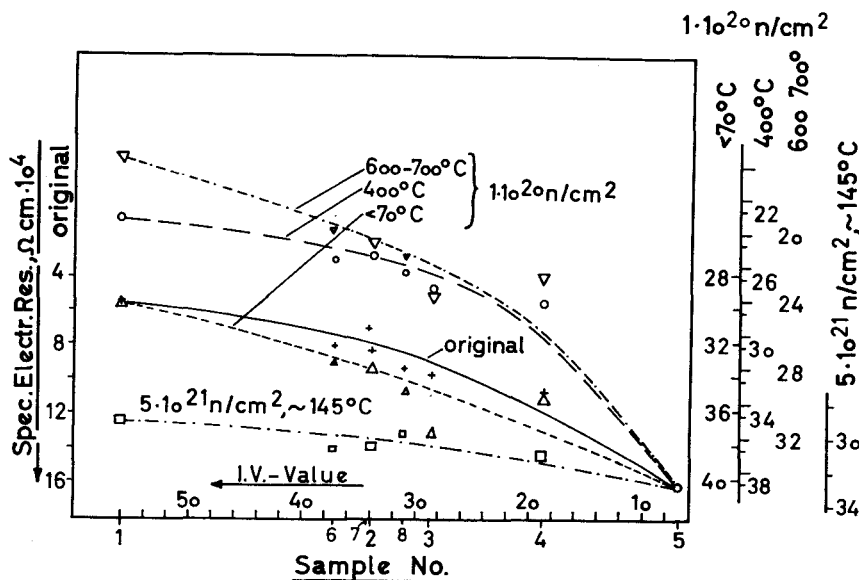


FIG. 12. Variation of the specific electrical resistance (with grain) by irradiation.

low-temperature irradiations the differences in the original graphites also are leveled out, but to a smaller extent than the differences in thermal conductivity. There do remain small differences in the electrical resistance even after an intensive irradiation of

samples, however, it is slightly decreased.

I. Strength Properties

The variations of properties under irradiation discussed so far show a dependence on the degree of graphitization of the samples

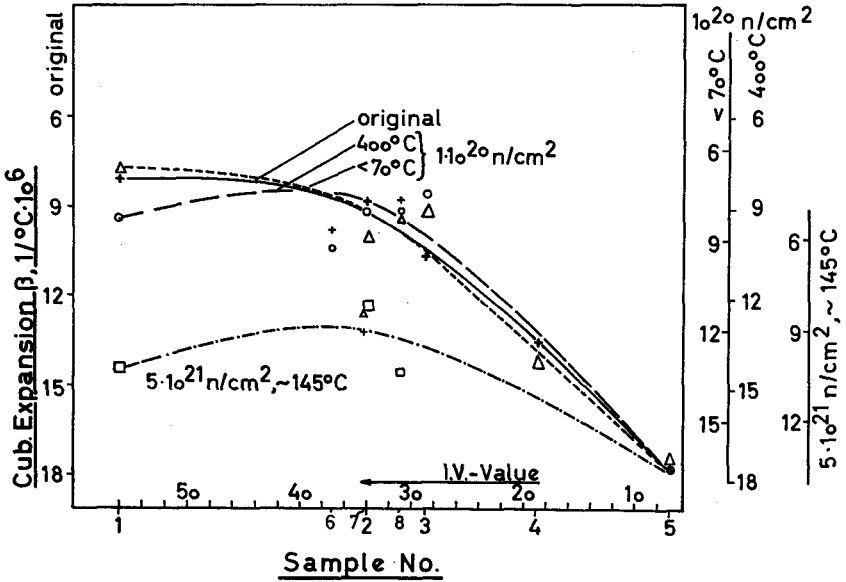


FIG. 13. Variation of the coefficient of cubical thermal expansion by neutron irradiation.

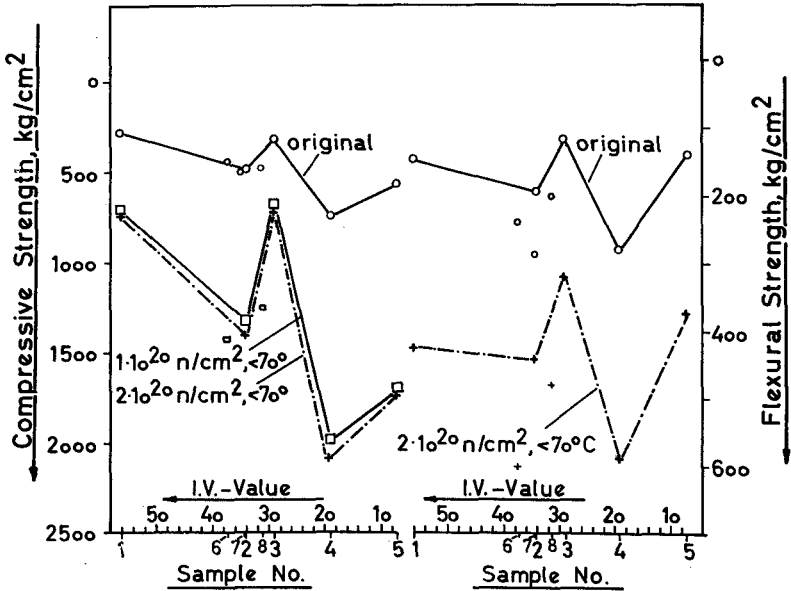


FIG. 14. Variation of the compressive and the flexural strength by neutron irradiation.

the flexural and compressive strengths plotted in Fig. 14, however, are independent of it. While all the strengths increase almost proportionately, each sample retains its individual characteristics.

For Young's Modulus determined by elastic

vibrations, the results are very similar. The Young's Moduli are increased by a factor of 3.

From these investigations it can be seen that with irradiation the samples undergo mechanical property changes which are largely independent of the filler materials.

The relative quality of the binder-bridges of the individual specimens remains unchanged even after quite different irradiation treatments. There is no difference in the effect of irradiation on the relative binding strength between the grains made of different cokes in artificial graphites.

#### IV. CONCLUSIONS

From these studies we can say, that irradiation in almost all cases levels out the differences in the degree of graphitization resulting from the use of different raw materials. Thus, the differences in those properties which are essentially caused by the filler disappear largely.

The leveling influence of irradiation,

however, is ineffective in the case of those factors which are predetermined by the binding properties. Therefore the relative differences in the strengths remain largely unchanged for irradiated specimens.

The experiments will be continued.

The authors are indebted to the Ministry of Atomic Affairs for sponsoring these studies.

Our thanks are also due to Professor Kersten and his co-workers, Institut für Reaktorwerkstoffe der Kernforschungsanlage Jülich, Aachen, for their help concerning the irradiations and for carrying out various physical measurements, and to Professor Knappwost and his co-workers, Institut für Physikalische Chemie der Universität Hamburg, for measuring the magnetic susceptibility, as well as to S.E.R.A.I. and especially to Dr. Ruston, Brussels, for providing the density values.